Polymer Testing 74 (2019) 178–186

Contents lists available at ScienceDirect

Polymer Testing

journal homepage: www.elsevier.com/locate/polytest

Material Properties

Testing the mechanical and tribological properties of new metal-polymer nanocomposite materials based on linear low-density polyethylene and $Al_{65}Cu_{22}Fe_{13}$ quasicrystals

I.E. Uflyand[a,*], E.G. Drogan[b], V.E. Burlakova[b], K.A. Kydralieva[c], I.N. Shershneva[d], G.I. Dzhardimalieva[c,d]

[a] Department of Chemistry, Southern Federal University, Rostov-on-Don, 344006, Russia
[b] Department of Chemistry, Don State Technical University, Rostov-on-Don, 344010, Russia
[c] Moscow Aviation Institute (National Research University), Moscow, 125993, Russia
[d] Institute of Problems of Chemical Physics, Russian Academy of Sciences, Chernogolovka, Moscow Region, 142432, Russia

ARTICLE INFO

Keywords:
Friction
LLDPE
Metal-polymer nanocomposite
Quasicrystals

ABSTRACT

Metal-polymer nanocomposite materials based on linear low-density polyethylene (LLDPE) and $Al_{65}Cu_{22}Fe_{13}$ quasicrystals were first obtained by melt-blending. The methods of thermal analysis and dynamic mechanical analysis were used to analyze the thermal stability and physicomechanical properties of the obtained nanocomposite materials. It has been found that increasing the content of nanofillers increases the elastic modulus, but tensile strength also increases, especially at low filler concentrations. Friction and wear were assessed on pin-on-disc tester. The results show that the friction coefficient of the sample with 1 wt% content of nanofiller is lower than that of pure LLDPE, and the anti-wear properties of the composite material are increased by 57% compared to pure LLDPE. In addition, during friction with a load of up to 147 N, a protective antifriction film of metallic nanoparticles on the friction surface forms for this sample.

1. Introduction

The main advantages of polymer-based composites as a matrix are high chemical resistance, good strength characteristics, low weight, low friction coefficient, and high wear resistance characteristic of polymers [1]. In this regard, extensive research is being conducted on the search for new polymer-filler combinations, which make it possible to obtain promising composite materials with improved functional properties [2]. Among composite materials for various purposes, materials based on filled polyolefins, which have high technological characteristics, low specific weight and low cost, are of particular interest. Currently, considerable attention is paid to nanocomposite materials with a number of important characteristics: less weight due to the low filler content; low cost due to the small amount of filler used; improved properties (including mechanical, thermal, electrical, magnetic, optical and other properties), etc. [3].

The development of highly efficient thermoplastic composite materials containing various functional nanofillers and processed into products using high-performance technologies is an urgent scientific and technical problem [4–6]. The method of mixing reagents used to obtain this type of composites has proven its effectiveness [7]. For its implementation are used extrusion, injection molding and extrusion, which reduces production time and cost of materials. This process is also environmentally friendly.

Quasicrystals (QCs), first discovered in 1984 [8], are complex metal alloys with a number of interesting physical properties [9–13], including stability up to the melting point [14], low friction coefficient (0.05–0.2) [15,16], high hardness ($HV_{0.2} \sim 800$) [17–19], low surface energy (~25 mJ/m^2) [20], high corrosion resistance [21] and high wear resistance [22]. The name of the quasicrystal is derived from the unique rotational symmetries arising due to its aperiodic atomic structure. After their discovery, it was found that the QC phases are contained in several hundred alloys [23]. The unusual combination of thermal, optical, and electrical properties of QCs made it possible to use them in many interesting applications [13,24–30]. The main disadvantage of QCs, which prevents their wide practical application, is low fracture toughness (about 0.5–3.5 MPa m½), whereas for metallic materials it exceeds 40 MPa m½ [19.27, [31,32]. It should also be noted that the low toughness and resistance to crack propagation at temperatures below 450 °C limit the use of QCs in the form of bulk parts

* Corresponding author. Department of Chemistry, Southern Federal University, 105/42 B. Sadovaya str., 344006, Rostov-on-Don, Russia.
E-mail address: ieuflyand@sfedu.ru (I.E. Uflyand).

https://doi.org/10.1016/j.polymertesting.2019.01.004
Received 6 November 2018; Received in revised form 2 January 2019; Accepted 6 January 2019
Available online 08 January 2019
0142-9418/

and thick-film coatings. These shortcomings can be successfully overcome by creating polymer-based composites filled with QCs [33–43]. The use of Al-Cu-Fe QCs as fillers can significantly improve the physical, mechanical, tribological, and thermal properties of composites with polymer matrices [38,44–50]. In particular, polymers filled with Al-Cu-Fe QCs have demonstrated wear resistance and improved mechanical properties due to hard fillers with a low aspect ratio [44,45,47]. In addition, QC powder in the polymer matrix almost does not cause abrasion to the steel counter face materials during wear tests [47,51]. Among the most interesting examples of Al-Cu-Fe QC-filled polymers, we note the composites based on epoxy resin [38,44,52], ultra-high molecular weight polyethylene (UHMWPE) [45,47,53], polyamide [46], high-density PE [54,55], polytetrafluoroethylene [56], ethylene-vinyl acetate [57], ethylene-tetrafluoroethylene [48,58], polyphenylene sulfide [38,59], and others.

Earlier, we developed three methods for producing quasicrystalline nanocomposites: from low-dimensional QC powders and film-forming polymers, by the forming QC *in situ* during thermal decomposition of the corresponding precursors and by thermal polymerization of the metal-containing monomers (QC components) with subsequent controlled pyrolysis of the formed metallopolymers [60]. These composite materials have radiation-protective properties against β-radiation [61,62]. A high correlation was found between the transmitted β-radiation and the relative dielectric constant of a composite material based on thermoplastic polymer matrices with a metal-containing filler.

The present paper is a continuation of this study and is devoted to the production of nanocomposite materials based on linear low-density polyethylene (LLDPE) and QCs, as well as the investigation of their physicomechanical and tribological properties.

2. Experimental

2.1. Materials

LLDPE 3306 WC4 grade with an MFI of 2.8 g/10 min and a density of 0.918 g/cm^3 (Taiwan) was used without further purification. The initial powder $Al_{65}Cu_{22}Fe_{13}$ (0.01 μm < d < 3 μm, distribution maximum 0.5 μm), obtained by the rapid crystallization method [24], was provided by the Federal State Unitary Enterprise VIAM (Russia).

2.2. Preparation of nanocomposites and nanocomposite films

Nanocomposite materials were obtained by mixing LLDPE and nanofiller using a compounder-extruder HAAKE Minilab (Rheomex CTW5) with synchronous rotation of two conical screws in an argon atmosphere. For example, to obtain 8 g of a nanocomposite, 5 g of polymer and powdered filler were loaded into an extruder. After receiving the first molded batch, an additional 3 g of all components of the mixture was added in proportion to the content of the filler from 0.1 to 20 wt.%. The experimental conditions were as follows: the extrusion temperature was 150 °C; the screw rotates at a speed of 60 rpm and 20 rpm when loading material; mixing time was 10–20 min; the temperature of the injection cylinder was 150 °C: the temperature of the injection mold was 80 °C; extrusion piston pressure was 300 bar; the time of extrusion of the material into the mold was 10 s. Subsequent automatic pressing was carried out for 10 s and the sample was removed from the mold. An electric manual hydraulic press was used to make films by hot pressing from blanks made in an injection molding machine. A nominal amount of composite materials was loaded into a polished flat mold into a gasket 0.2 mm thick. To prevent adhesion, fluoroplastic film was used. The mold was heated to 150 °C. The heating rate of the blanks was controlled by a laboratory automatic transformer RNO-250-2 (LAT) (I = 8 A), which regulates the supply voltage in the range of 0–220 V. The temperature was controlled by a thermoelectric thermometer KVP1-511 with an iron-copper-nickel thermocouple, type J. After reaching the required temperature, the mold was compressed under 150 atm. The films were removed after cooling the mold to 50 °C. The obtained composite film with a size of 0.2 × 100 × 100 mm was used for physicomechanical tests.

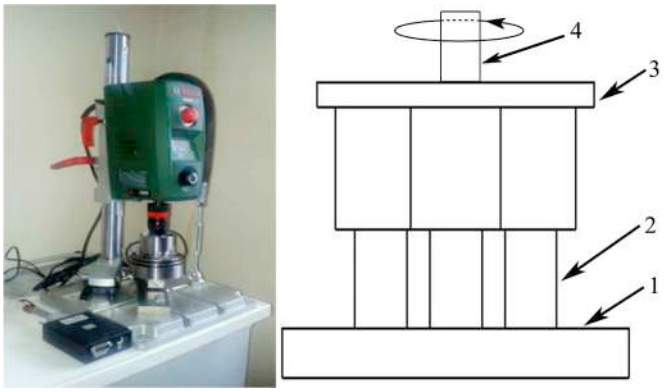

Fig. 1. Setup for tribological tests: (left) universal testing machine UMT-200; (right) pin-on-disk tribo-testing geometric configuration: 1 - LLDPE sample, 2 - steel pins, 3 - holder, 4 - axis of rotation.

Table 1
Polymeric nanocomposite materials and their preparation conditions.

Sample	The original ratio of components, wt. %		Extrusion mode		
	Quasicrystal	Polymeric matrix	Number rpm	t, °C	Time, min
1	0.1	99.9	60	150	20
2	0.5	99.5	60	150	20
3	1.0	99.0	60	150	20
4	3.0	97.0	60	150	20
5	5.0	95.0	60	150	20
6	10.0	90.0	60	150	20

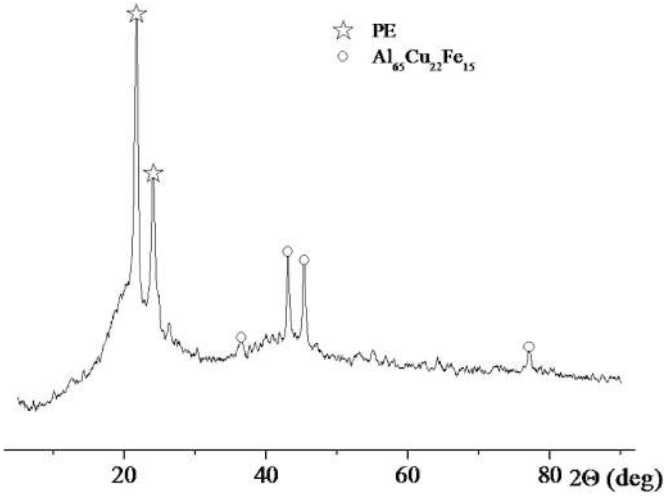

Fig. 2. X-ray diffractogram of sample **6**.

2.3. Characterizations

X-ray diffraction (XRD) analysis was performed on a DRON-UM-2 powder diffractometer with CuKα radiation (λ_{Cu} = 1.54184 Å) in the angle range 2θ = 5-80° with a scanning speed of 5 deg/min and a temperature of 25 °C to determine the phase composition and size of crystallites. Particle size was calculated based on the extension of the lines in the spectrum in accordance with the Debye-Scherer equation (1) [63]:

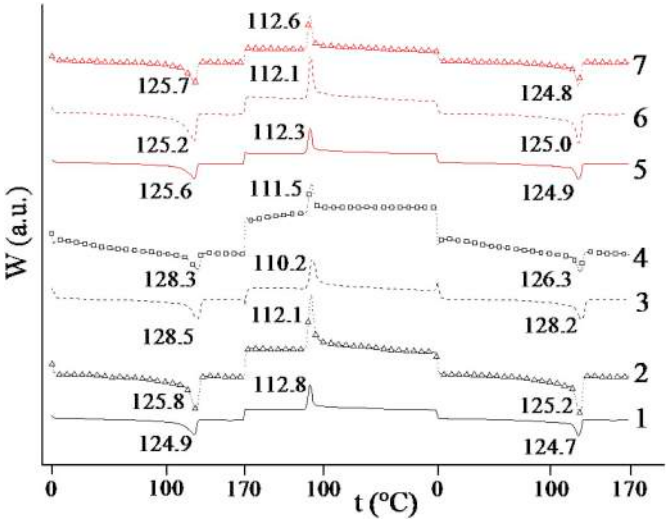

Fig. 3. DSC curves for LLDPE (1) and nanocomposites with a filler concentration (wt.%): 0.1(2), 0.5(3), 1(4), 3(5), 5(6), 10 (7).

Table 2
Temperature, heat of melting and crystallinity of nanocomposites.

Sample	t_m, °C	ΔH_m, J/g	$\Delta\chi$, %
LLDPE	124.7	119	42
1	125.2	117	41
2	128.2	107	37
3	126.3	87	30
4	124.9	115	40
5	125.0	110	39
6	124.8	78	27

Table 3
Physicomechanical properties of nanocomposite materials.

Sample	*E*, GPa	σ_{fr}, MPa	ε, %
Condition I (injection-molding machine, 1.85-mm-thick blank)			
LLDPE	0.08 ± 0.01	14.7 ± 3.2	203 ± 42
1	0.16 ± 0.02	16.0 ± 1.1	211 ± 37
2	0.15 ± 0.02	17.1 ± 0.7	287 ± 54
3	0.08 ± 0.01	18.9 ± 2.5	419 ± 34
4	0.18 ± 0.01	16.8 ± 1.8	305 ± 42
5	0.16 ± 0.03	17.6 ± 0.4	250 ± 36
6	0.15 ± 0.03	17.6 ± 1.4	265 ± 41
Condition II (hot pressing, 0.21-mm-thick film)			
LLDPE	0.32 ± 0.01	21.8 ± 2.7	1018 ± 115
2	0.30 ± 0.01	17.5 ± 4.2	897 ± 30
4	0.29 ± 0.01	20.0 ± 2.6	1045 ± 98
6	0.30 ± 0.01	17.6 ± 4.2	921 ± 24

$$d = \frac{K \cdot \lambda}{\beta \cos\theta}, \quad (1)$$

where d is the average size of domains (crystallites); K is the dimensionless particle shape factor (the Scherer constant is ~0.9); β is the peak width (at half maximum intensity); λ is the X-ray wavelength; θ is the diffraction angle.

Thermogravimetric (TG) studies and differential scanning calorimetry (DSC) analysis of the composites were performed using TGA Q500 V6.7 Build 203 and Mettler DSC 30 meters with a heating rate of 10 deg/min. For a quantitative measurement of the thermal effects of reactions occurring in the samples and the simultaneous evaluation of the weight change, a synchronous thermal analyzer STA 409C Luxx was used, coupled with a QMS 403C Aeolos quadrupole mass spectrometer, NETZSCH (Germany). The measurements were carried out in a nitrogen atmosphere (60 mL/min).

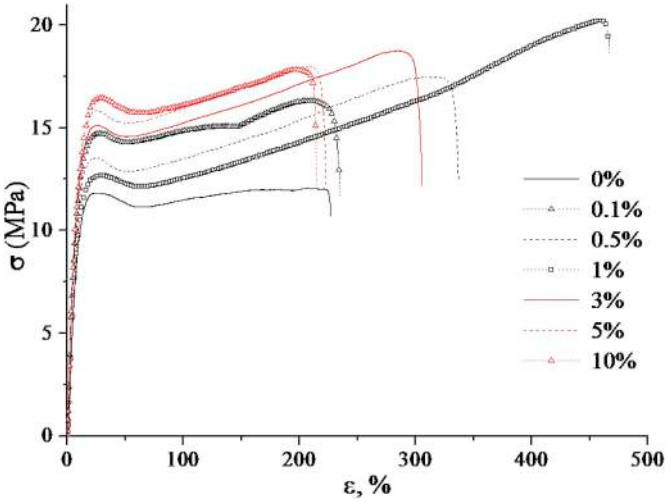

Fig. 4. Stress-strain curves for the initial LLDPE and nanocomposites with different filler contents.

The physicomechanical properties were studied on the universal Zwick/Roel Z010 TCFR010TH machine under rupture conditions at a speed of 5 mm/min. The tests were carried out using two types of blades. Samples with a thickness of 1.85 mm were obtained in accordance with ISO 527-2-5A standard using the HAAKE MiniJet injection machine. Blades 0.2 mm thick were cut out using a hand press from a film after thermal molding. Results were averaged for at least 5 samples. The test included a measurement of the tensile modulus *E*, MPa, fracture stress σ_{fr}, MPa, fracture strain ε_{fr}.

Measurements of the dynamic mechanical properties of polyethylene samples were carried out using a dynamic mechanical analyzer DMA 242C (Netzsch-Gerätebau GmbH, Germany) in a two-arm bending mode with a free sample length of 2 × 5 mm, as well as in the uniaxial tension mode of a sample of 20 × 6 × 0.2 mm with continuous scanning temperature from −170 to 150 °C at a rate of 2 deg/min in a helium atmosphere. A sinusoidal oscillatory force was applied to the samples, allowing to develop a maximum strain amplitude of 30 μm at three fixed frequencies of 0.1, 1, and 10 Hz. Samples were investigated for the components of the modulus of complex dynamic properties - the storage modulus (E′), the loss modulus (E"), and the loss tangent (tgδ) for bending and stretching mode.

Tests for crack resistance were carried out in three-point bending mode on samples of pure polymer and composite. The test specimen was selected in accordance with the standard test method ASTM D5045-99 to determine the viscosity of flat strain at break and the rate of release of strain energy, providing conditions for flat strain with a nominal sample size such as 3 × 6 × 24 mm^3. In accordance with the ASTM standard, the crack length was chosen so that the ratio between the crack width and the crack length was in the range of 0.45–0.55.

Antifriction and anti-wear characteristics were performed on a universal testing machine (Fig. 1, left) of the UMT-200 type (Research and Production Center “Konvers-resurs”, Russia) with the pin-on-disc arrangement. The friction unit consisted of a rigidly fixed annular sample in the form of a disk made of LLDPE with the addition of QC nanopowders of various concentrations and three moving steel pins arranged around a circle at an angle of 120° to each other (Fig. 1, right). Before testing, the steel samples were cleaned with abrasive paper, degreased with hexane and dried in air. Samples from LLDPE were weighed before and after tribological tests on an analytical balance, and wear was determined from the weight loss of the sample. Tribological studies were carried out at a temperature of 25°C with a consistent increase in load (47N, 98N and 147N) with a rotation speed of 25 rpm, the total linear distance was approximately 2250 m. The change in friction coefficient was recorded using QMLab software.

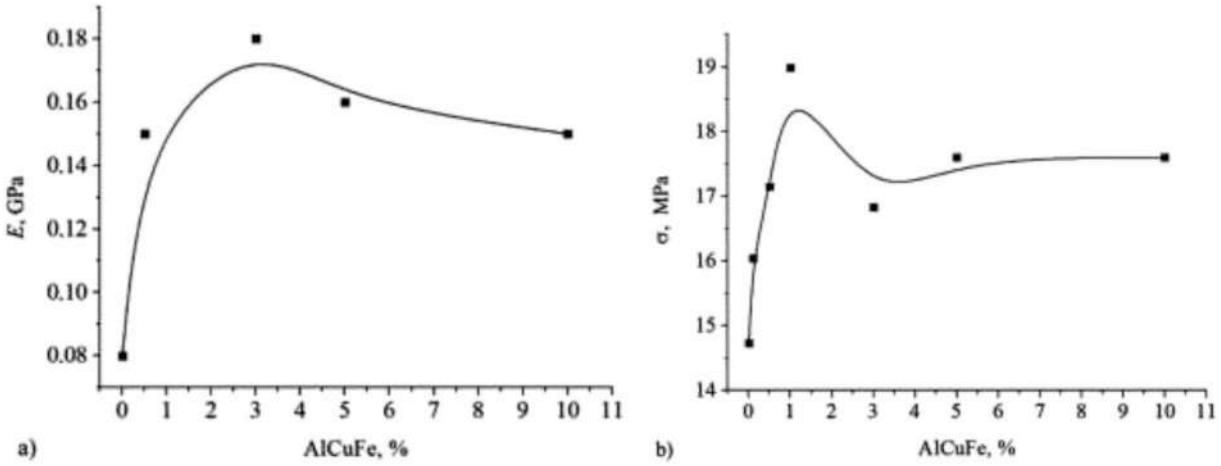

Fig. 5. The dependence of the elastic modulus (a) and tensile strength (b) of the nanocomposite on the filler content.

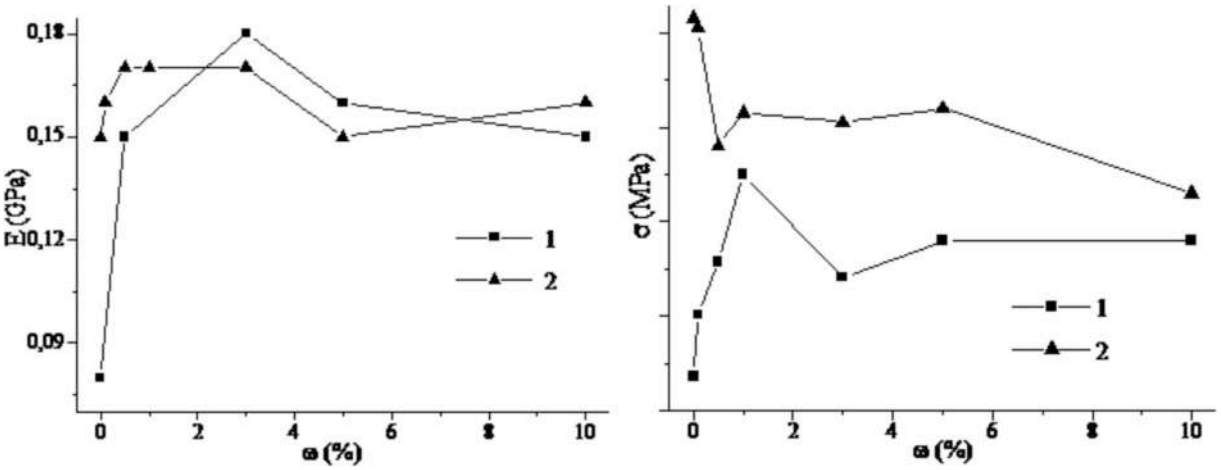

Fig. 6. The dependence of the elastic modulus (left) and tensile strength (right) on the filler content for nanocomposites obtained at temperatures of 150 (1) and 300°C (2).

Table 4
Dynamic mechanical analysis of nanocomposites in the mode of double shoulder bending in the temperature range of −170…150°C at a measurement frequency of 1 Hz.

Sample	E' (22°C), MPa	t_1, °C		$tg\delta_1$ (peak)	t_2, °C by E" peak	t_3, °C by tgδ peak	t_m, °C by onset E'	
		by E" peak	by tgδ peak				by onset lgE′	by tgδ peak
LLDPE	165	−133	−120	0.073	−31	86	116	125
1	217	−136	−124	0.116	−27	94	116	125
2	196	−138	−124	0.115	−26	83	117	126
3	213	−133	−122	0.087	−26	89	116	126
4	199	−140	−122	0.090	−27	83	117	132
5	187	−149	−126	0.114	−28	77	116	127
6	200	−142	−126	0.124	−32	86	117	126

Table 5
Dynamic mechanical analysis of nanocomposites for uniaxial tension in the temperature range −170…150 °C at a measurement frequency of 1 Hz.

Sample	E' (T = 22°C), MPa	T_1, °C		$tg\delta_1$ (peak)	T_2, °C by E" peak	T_m, °C by onset E′	
		by E" peak	by tgδ peak			by onset lgE′	by tgδ peak
LLDPE	637	−158	−141	0.095	−44	124	122
2	685	−145	−127	0.054	−56	126	123
4	630	−145	−128	0.051	−43	125	–
6	681	−140	−132	0.053	−50	126	115

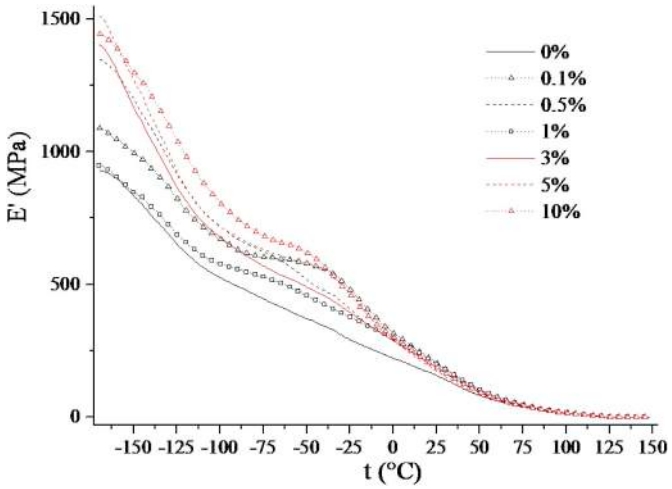

Fig. 7. Temperature dependences of the elastic modulus at a frequency of 1 Hz for film samples in the range of −170…150 °C: LLDPE (1) and nanocomposites with filler content (wt.%): 0.1 (2), 0.5 (3), 1 (4), 3 (5), 5 (6), 10 (7).

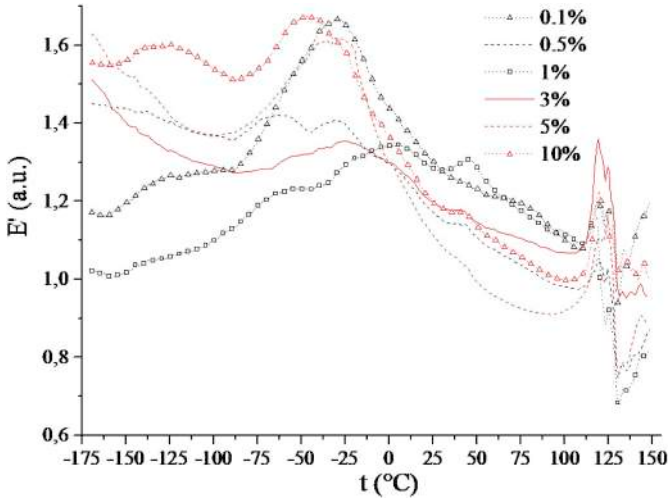

Fig. 8. Temperature dependences of the relative modulus of elasticity at a frequency of 1 Hz of film samples in the range of −170…150 °C for nanocomposites with filler content (wt.%)): 0.1 (1), 0.5 (2), 1 (3), 3 (4), 5 (5), 10 (6) in bending mode.

3. Results and discussions

3.1. Preparation, morphology and microstructure of nanocomposites

The polymer shell separates the metal particles from each other and from the external environment and, thus, performs the function of a stabilizer and improves the properties of the metal-polymer composite. To obtain such nanocomposites, various methods are used: coacervation, deposition by a nonsolvent or evaporation of a solvent, physical adsorption, extrusion (the particles of covered with the shell upon forcing of the quasicrystalline intermediate compound through the film-forming material), sputtering in a fluidized bed, condensation of a vapor, polymerization on the particle surface, and others. Technologically more attractive are the methods of mechanochemical mixing of a metal alloy together with a polymer matrix. Depending on the nature of the movement of the ball load (polished metal or agate balls), three modes of grinding the polymer matrix are realized: sliding (abrasion), rolling (impact) and vortex (mainly impact). Under the action of shock and shear loads, not only dispersion occurs, but also the effective introduction of filler particles into a polymer matrix. In this

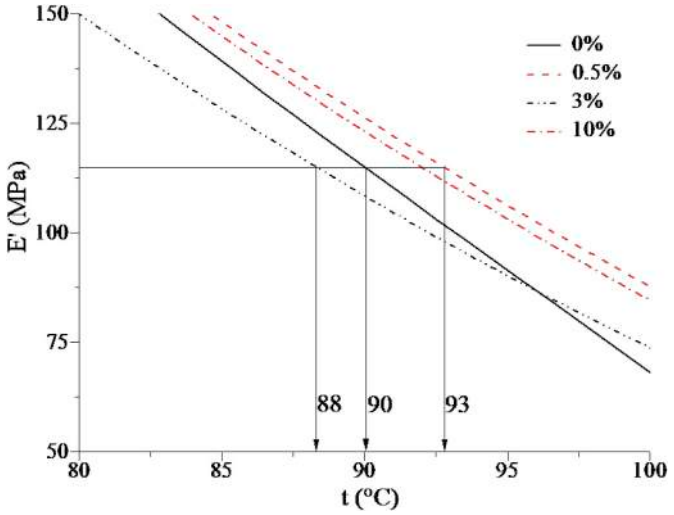

Fig. 9. Temperature dependences of the tensile modulus at a frequency of 1 Hz for film samples in the temperature range 70...110 °C: LLDPE (1) and nanocomposites with filler content (wt.%) 0.5 (2), 3 (3), 10 (4).

work, we used a method for producing composite materials with the $Al_{65}Cu_{22}Fe_{13}$ alloy based on a thermoplastic LLDPE by mixing in a polymer melt using a twin-screw extruder, which is an efficient processing method and may play an important role in obtaining a nanocomposite with uniform microstructure. Conditions and technological modes of obtaining nanocomposite materials are presented in Table 1.

The composition, morphology and microstructure of the obtained nanocomposite materials were studied by XRD analysis. When dispersing, the filler nanoparticles are fairly evenly distributed in the bulk of the matrix. In particular, both particles of initial sizes and their conglomerates are observed, which is also confirmed by wide peaks on XRD patterns corresponding to the phase of the nanofiller (Fig. 2). The appearance of other lines is not observed, which indicates the process of dispersion of the filler in the polymer matrix without phase transformations.

The introduction of fillers affects the structural state of nanocomposites. The DSC data (Fig. 3) indicate a systematic decrease in the enthalpy of melting ΔH_m with an increase in the content of nanoparticles of the $Al_{65}Cu_{22}Fe_{23}$ alloy in the LLDPE polymer matrix.

The dependences of crystallinity ($\Delta\chi$) of nanocomposites, calculated by formula (2), have a similar character:

$$\Delta\chi = [(\Delta H_m - \Delta H_o)/\Delta H_o]x100 \quad (2)$$

where ΔH_m is the heat released during the melting of the sample, ΔH_o is the heat released during the melting of 100% crystalline polymer (for LLDPE, $\Delta H_o = 285$ J/g).

The decrease in the degree of crystallinity of the filled LLDPE compared to LLDPE (Table 2) is probably due to the formation of a less ordered crystalline structure.

It is known that the influence of inorganic particles on the cry stallization process of polymers is determined by a number of factors, including the size of the filler particles and their size distribution, the effective surface of the particles, the degree of interaction between the polymer and the filler particles, the degree of crystallinity of the original polymer matrix. Depending on these factors, filler particles can bind polymer chains (reduce crystallinity) or act as nucleation centers (increase crystallinity). In the case of $Al_{65}Cu_{22}Fe_{15}$/LLDPE nanocomposites under consideration, the introduced filler particles are mainly localized in the amorphous regions of the polymer molecule. Taking into account the relatively low degree of crystallinity of the initial LLDPE and due to the steric and kinetic difficulties of macromolecular mobility, the introduction of fillers into the polymer melt leads to a decrease in crystallinity, which also agrees with known

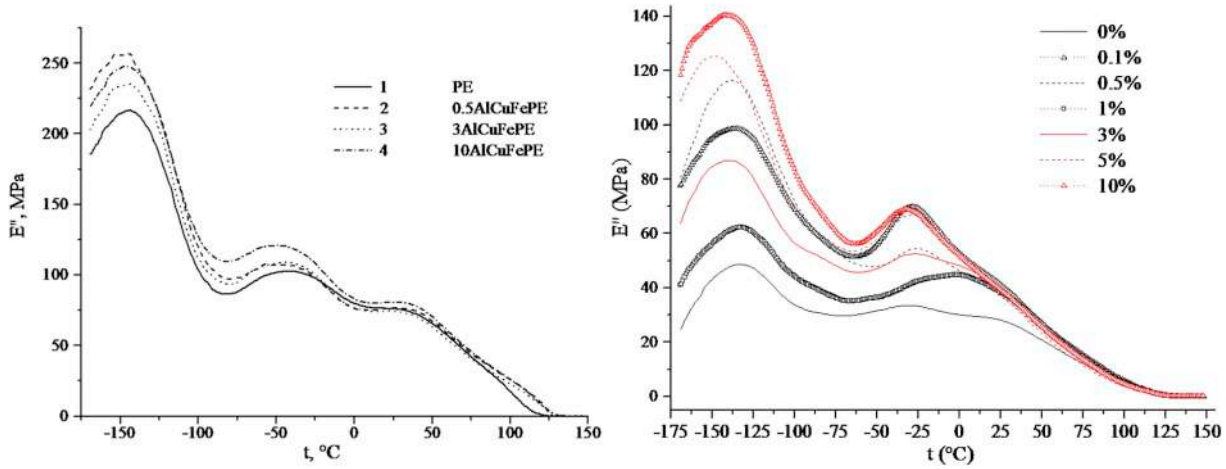

Fig. 10. Temperature dependences of the loss modulus at a frequency of 1 Hz for film samples in the temperature range of −170…150 °C: LLDPE (1) and nanocomposites in tensile mode (a) and bending (b) with filler content (wt.%): 0.1 (2), 0.5 (3), 1 (4), 3 (5), 5 (6), 10 (7).

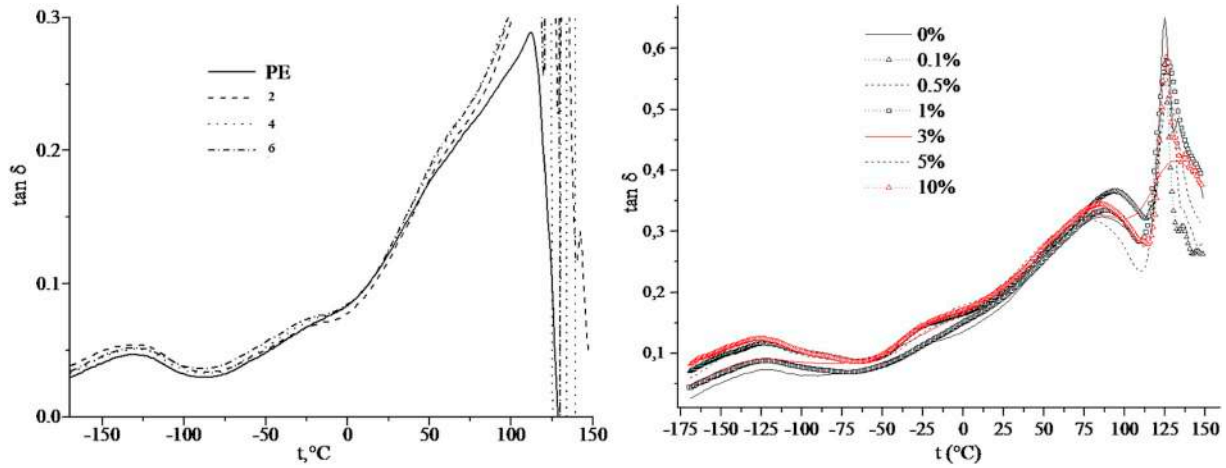

Fig. 11. Temperature dependences of the loss tangent at a frequency of 1 Hz for film samples in the temperature range of −170...150 °C: LLDPE (1) and nanocomposites in tensile mode (a) and bending (b) with filler content (wt.%) 0.1 (2), 0.5 (3), 1 (4), 3 (5), 5 (6), 10 (7).

literature data [64].

3.2. Physicomechanical properties of nanocomposites

Samples of the film of nanocomposite materials were obtained in two modes by casting using an injection-molding machine (film thickness 1.85 mm) or hot-pressing (film thickness 0.21 mm). As follows from the physicomechanical characteristics of nanocomposite films, the presence of a quasicrystalline melt as a filler improves the strength properties in the LLDPE-$Al_{65}Cu_{22}Fe_{13}$ system, which is most typical of the samples obtained under conditions I (Table 3, Fig. 4).

With an increase in the filler content, the elastic modulus as well as the tensile strength increase, especially at low filler concentrations (Fig. 5).

The dependences obtained are consistent with the literature data. For example, for the UHMPE-quasicrystalline Pt-Zr melt system, it was shown that the introduction of a metal alloy significantly increases the wear resistance of the composite material [65]. It is obvious that the improvement of the viscoelastic characteristics of a polymer composite material in the presence of a quasicrystalline filler, along with an increase in its elastic modulus and preservation of the damping properties of the polymer matrix, may be of interest for using such composites as wear-resistant coatings, surface components of friction products, etc.

To study the effect of various technological regimes of obtaining nanocomposite materials on their properties, nanocomposites were obtained at two temperatures of 150 and 300 °C. Fig. 6 shows the dependence of the elastic modulus and tensile strength on the filler content in nanocomposites obtained at different temperatures.

The nature of the dependence of the elastic modulus on the change in the content of the filler in the $Al_{65}Cu_{22}Fe_{15}$/LLDPE system is supported for different temperature regimes, although for both the native polymer and nanocomposites with a low filler content the E values increase by 10–12%. Probably, this behavior may be associated with the structuring of the polymer matrix at higher synthesis temperatures. For products of the high-temperature regime, there is also a general tendency that the strength characteristics of the analyzed nanocomposites depend on the filler content, although here the tensile strength exceeds those of nanocomposites obtained at 150 °C. In general, given that the process of obtaining nanocomposites at high temperatures is accompanied by undesirable crosslinking reactions of the polymer matrix, its partial destruction, as well as higher energy consumption, low temperature regime is most optimal for obtaining the nanocomposites of the considered types.

Measurements of the dynamic mechanical properties of the samples were carried out in the temperature range from −170 to 150°C at frequencies of 0.1, 1 and 10 Hz. A characteristic parameter in dynamic mechanical studies is the loss coefficient (tanδ), which is determined from the relationship:

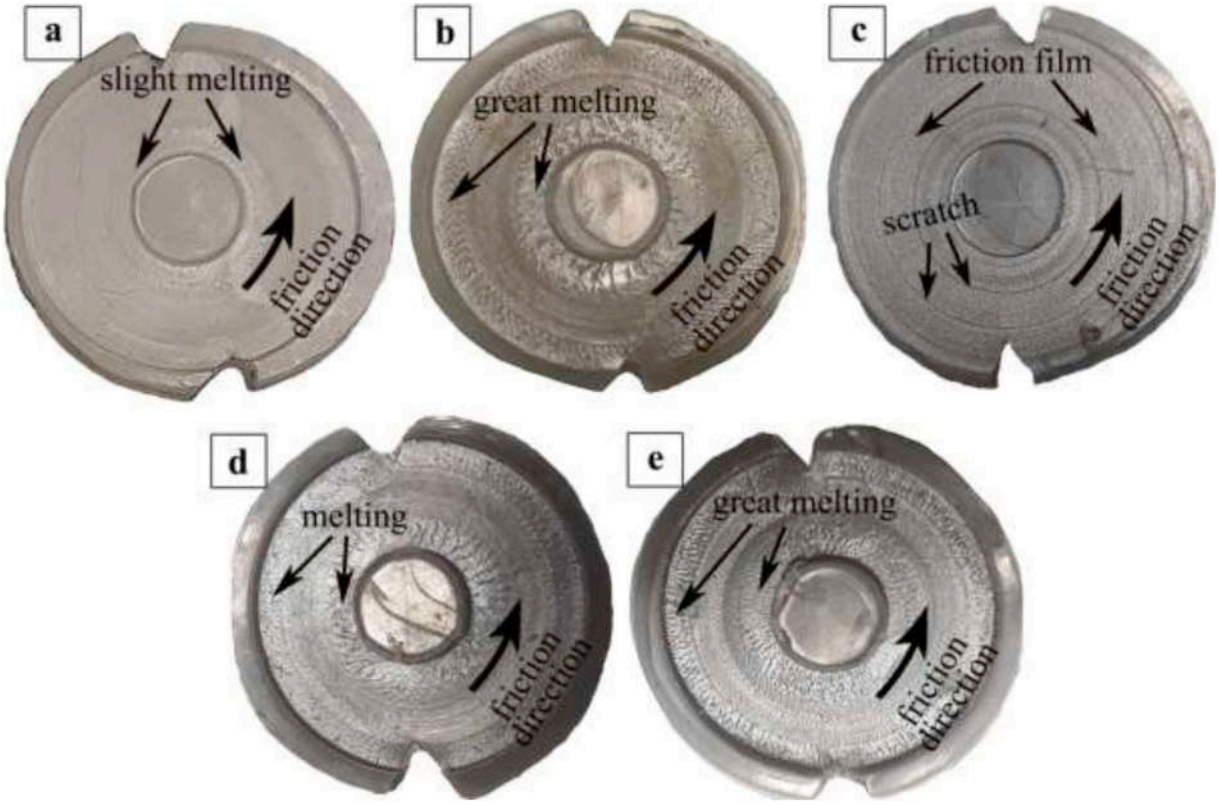

Fig. 12. Image of the surface of samples after friction at P = 147 N: a – LLDPE, b – sample **1**, c – sample **3**, d – sample **5**, e – sample **6**.

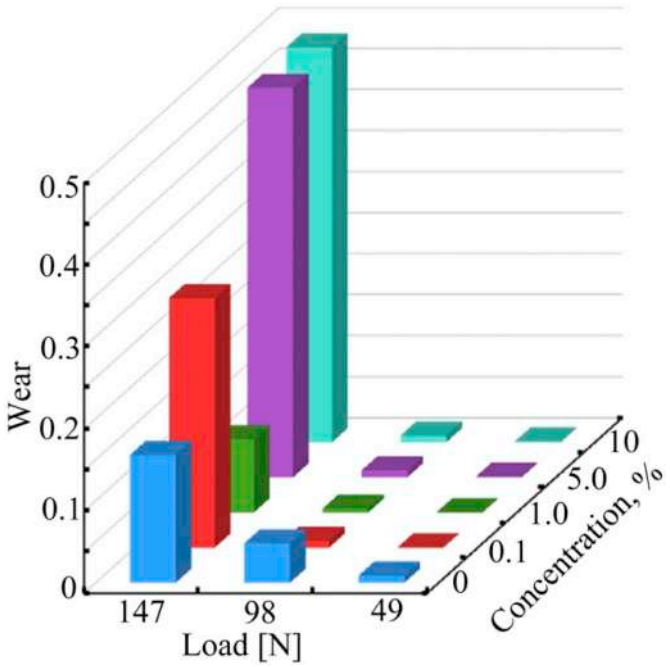

Fig. 13. Dependence of anti-wear characteristics of pure LLDPE (on the concentration axis - "0") and LLDPE with the addition of QC nanoparticles of various concentrations (on the concentration axis - "0.1, 1.0, 5.0, 10") on axial load.

$$\mathrm{tg}\delta = \frac{E''}{E'}, \tag{3}$$

where E′ is the storage modulus, E" is the loss modulus, δ is the phase shift between the applied sinusoidal force and deformation.

The dynamic modulus of elasticity of composites E′ exceeds the

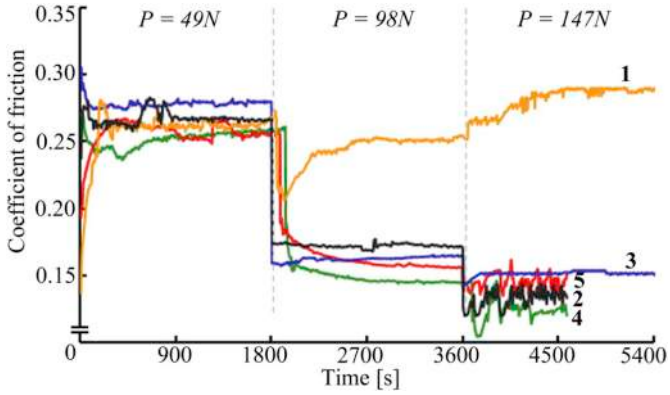

Fig. 14. Evolution of the friction coefficient with time with increasing load: 1 – LLDPE, 2 – sample **1**, 3 – sample **4**, 4 – sample **5**, 5 – sample **6**.

modulus of unfilled polyethylene in a wide range of temperatures (Tables 4 and 5, Fig. 7).

An increase in the filler content is accompanied by a significant increase in the dynamic modulus of elasticity of the material in the temperature range 20–40 °C. Thus, at 22 °C, E′ of sample **6** is increased by 29% compared to the unfilled polymer. This behavior of elastic dynamic mechanical properties indicates a sufficient level of intermolecular interactions between the polymer molecule and the surface of the nanofiller. With an increase in temperature, the introduction of fillers leads to an increase in the elastic modulus in the regions of relaxation transitions (Fig. 8), which is caused by a decrease in the modulus of the polymer matrix and, accordingly, an increase in the ratio of the modulus of the filler to the modulus of the matrix ($E'_{rel} = E'_f/E'_{PE}$).

A change in the dynamic modulus at high temperatures provides information on the heat resistance of the material (Fig. 9). The value of

the modulus of unfilled polyethylene corresponding to a temperature of 90 °C (the beginning of amorphization of PE) for a nanocomposite with a filler content of 20 wt.% is supported up to 99 °C, indicating a slight increase in the heat resistance of the material, although its content is 3 wt.%.

The temperature dependences of the modulus and tangent of the angle of mechanical loss of LLDPE composites show characteristic transitions of α-, β-, and γ-relaxation associated with movements in the amorphous and crystalline parts of polyethylene (Figs. 10 and 11). The introduction of fillers does not have a noticeable effect on transition temperatures; at low concentrations, a small increase in the α-transition temperature is observed from 86 to 94 °C for sample **1**, but an increase in the intensity of the peak of temperature transitions is observed in the entire concentration range studied. Since the α-transition is mainly associated with the movement of chain links in the crystalline phase of the polymer, the shift of the α-transition peak towards higher temperatures may be due to an increase in the crystallinity of the material and crystallite size, which is consistent with a higher degree of crystallinity of the nanocomposite **2**.

It is believed [66] that β-relaxation is responsible for large-scale movements of polymer molecules in the region of the amorphous phase. As follows from the data of Tables 4 and 5 and Fig. 9, the dependence of β-relaxation on the composition of nanocomposites correlates with an increase in the total mobility of the amorphous phase and a decrease in the crystallinity of nanocomposite samples, with the exception of some nanocomposites with a low filler content. In samples of nanocomposites, the character of changes in β transitions is similar. For example, for samples **2** and **6**, the peak of β-relaxation shifts to low temperatures from −44 to −66 °C and from −44 to −50 °C, respectively. The position of the γ-transition, which is believed to be responsible for the joint motion of 3–4 methylene units in the amorphous regions of polymers, is in the range of −130…-142°C for the studied nanocomposites (see Tables 4 and 5).

3.3. Tribological tests

As shown by the results of tribological tests, the long-term frictional interaction of a friction pair LLDPE-steel contributes to an increase in temperature in the friction unit, which leads to the subsequent easy melting of the surface of the LLDPE sample (Fig. 12a). The addition of nanoparticles with a concentration of 0.1%, 5% and 10% to the organic matrix in LLDPE leads to a strong melting of the composite material as a result of friction (Fig. 12b, d, e). However, the addition of 1% QC nanoparticles in LLDPE apparently raises the melting point of the composite material, the sample becomes more resistant to thermal effects, and as a result of frictional interaction, an antifriction metal film is observed on the friction track (Fig. 12c).

The results of studies of the wear resistance of composite materials show that the addition of QC nanoparticles contributes to a decrease in wear compared to pure LLDPE under friction with loads of 49 N and 98 N for all the tested samples (Fig. 13). An increase in the load to 147 N leads to an increase in wear and serious destruction of samples with the addition of QC nanoparticles with a percentage concentration of 0.1, 5 and 10 compared to pure LLDPE. However, a sample of LLDPE with the addition of QC nanoparticles with a concentration of 1% withstands strong shear stresses and anti-wear properties of the composite material compared to pure LLDPE increased by 57%.

Studies of the antifriction characteristics of composite materials showed that the addition of QC nanoparticles to LLDPE leads to a decrease in the friction coefficient with increasing load, in contrast to pure LLDPE (Fig. 14). Increasing the load to 147 N for samples **2**, **4** and **5** leads to self-oscillations in the process of friction; the friction coefficient becomes unstable and leads to severe wear of the composite material (see Fig. 12), which is in the process of friction; there is a strong destruction of the material and the formation of wear products in the form of chips. On the contrary, an increase in the load to 147 N for sample **3** contributes to the stabilization of the friction coefficient and the formation of QC nanoparticles on the friction surface of the protective antifriction film.

4. Conclusions

Composite materials based on thermoplastic matrices of LLDPE and the quasicrystalline $Al_{65}Cu_{22}Fe_{13}$ alloy were obtained by mixing the components in the polymer melt. The developed technological regimes for obtaining new nanocomposite materials make it possible to effectively control their thermal, mechanical and tribological properties. A systematic decrease in the enthalpy of melting and the degree of crystallinity of nanocomposites with an increase in the content of $Al_{65}Cu_{22}Fe_{13}$ alloy nanoparticles in the LLDPE polymer matrix was established. The presence of a quasicrystalline alloy as a filler leads to an improvement in the strength properties of the composite material. The dynamic modulus of elasticity of composites exceeds the modulus of unfilled LLDPE in a wide temperature range. Tribological tests show that LLDPE filled with 1 wt.% QC nanoparticles shows a 57% reduction in weight compared to unfilled LLDPE.

References

[1] S.S. Pesetskii, S.P. Bogdanovich, N.K. Myshkin, Tribological behavior of nanocomposites produced by the dispersion of nanofillers in polymer melts, J. Frict. Wear 28 (2007) 457–475.

[2] N.T. Kakhramanov, A.G. Azizov, V.S. Osipchik, U.M. Mamedli, N.B. Arzumanova, Nanostructured composites and polymer materials science, Int. Polym. Sci. Technol. 44 (2017) 37–47.

[3] C. DeArmitt, R. Rothon, Particulate fillers, selection, and use in polymer composites, in: S. Palsule (Ed.), Polymers and Polymeric Composites: A Reference Series, Springer, Berlin, Heidelberg, 2016.

[4] J. Sun, J. Shen, S. Chen, M.A. Cooper, H. Fu, D. Wu, Z. Yang, Nanofiller reinforced biodegradable PLA/PHA composites: current status and future trends, Polymers 10 (2018) 505.

[5] S. Coiai, E. Passaglia, A. Pucci, G. Ruggeri, Nanocomposites based on thermoplastic polymers and functional nanofiller for sensor applications, Materials 8 (2015) 3377–3427.

[6] M. Šupová, G.S. Martynková, K. Barabaszová, Effect of nanofillers dispersion in polymer matrices: a review, Sci. Adv. Mater. 3 (2011) 1–25.

[7] T. Hanemann, D.V. Szabó, Polymer-nanoparticle composites: from synthesis to modern applications, Materials 3 (2010) 3468–3517.

[8] D. Shechtman, I. Blech, D. Gratias, J.W. Cahn, Metallic phase with long-range orientational order and no translational symmetry, Phys. Rev. Lett. 53 (1984) 1951–1953.

[9] S. Shaitura, A.A. Enaleeva, Fabrication of quasicrystalline coatings: a review, Crystallogr. Rep. 52 (2007) 945–952.

[10] F. Samavat, M.H. Tavakoli, S. Habibi, B. Jaleh, P.T. Ahmad, Quasicrystals, Open J. Phys. Chem. 2 (2012) 7–14.

[11] B.A.S.G. de Lima, R.M. Gomes, S.J.G. de Lima, D. Dragoe, M.-G. Bathers-Labousse, R. Kouitat-Njiwa, et al., Self-lubricated, low-friction, wear-resistant Al-based quasicrystalline coatings, Sci. Technol. Adv. Mater. 17 (2016) 71–79.

[12] R.T. Li, V.K. Murugan, Z.L. Dong, K.A. Khor, Comparative study on the corrosion resistance of Al–Cr–Fe alloy containing quasicrystals and pure Al, J. Mater. Sci. Technol. 32 (2016) 1054–1058.

[13] E. Huttunen-Saarivirta, Microstructure, fabrication and properties of quasicrystalline Al-Cu-Fe alloys: a review, J. Alloy. Comp. 363 (2004) 150–174.

[14] A.P. Tsai, A. Inoue, T. Masumoto, A stable quasicrystal in Al-Cu-Fe system, Jpn. J. Appl. Phys. 26 (1987) L1505–L1507.

[15] J.M. Dubois, P. Brunet, W. Costin, A. Merstallinger, Friction and fretting on quasicrystals under vacuum, J. Non-Cryst. Solids 334–335 (2004) 475–480.

[16] J.M. Dubois, S.S. Kang, A. Perrot, Towards applications of quasicrystals, Mater. Sci. Eng., A 179–180 (1994) 122–126.

[17] A.P. Tsai, H. Suenaga, M. Ohmori, Y. Yokoyama, A. Inoue, T. Masumoto, Temperature dependence of hardness and expansion in an icosahedral Al-Pd-Mn alloy, Jpn. J. Appl. Phys. 31 (1992) 2530–2531.

[18] R. Wittmann, K. Urban, Mechanical properties of single-quasicrystalline alcucosi, J. Mater. Res. 6 (1991) 1165–1168.

[19] U. Koester, W. Liu, H. Hertzberg, M. Michel, Mechanical properties of quasicrystalline and crystalline phases in Al-Cu-Fe alloys, J. Non-Cryst. Solids 153–154 (1993) 446–452.

[20] C.J. Jenks, P.A. Thiel, Surface properties of quasicrystals, MRS Bull. 22 (1997) 55–58.

[21] S.L. Chang, W.B. Chin, C.M. Zhang, et al., Oxygen adsorption on a single-grain, quasicrystal surface, Surf. Sci. 337 (1995) 135–146.

[22] Y. Chen, J. Qiang, C. Dong, Smearing-type wear behavior of $Al_{62}Cu_{25.5}Fe_{12.5}$ quasicrystal abrasive on soft metals, Intermetallics 68 (2016) 23–30.

[23] A.P. Tsai, “Back to the future” − an account discovery of stable quasicrystals, Acc. Chem. Res. 36 (2003) 31–38.

[24] Y.K. Vekilov, M.A. Chernikov, Quasicrystals, Physics-Uspekhi 53 (2010) 537–560.
[25] A. Thiel, J.M. Dubois, Quasicrystals. Reaching maturity for technological applications, Mater. Today 2 (1999) 3–7.
[26] M. Roy, Formation and magnetic properties of mechanically alloyed $Al_{65}Cu_{20}Fe_{15}$ quasicrystal, J. Magn. Magn Mater. 302 (2006) 52–55.
[27] E. Maciá, Optimizing the thermoelectric efficiency of icosahedral quasicrystals and related complex alloys, Phys. Rev. B 80 (2009) 205103.
[28] Y. Takagiwa, T. Kamimura, S. Hosoi, J.T. Okada, K. Kimura, Thermoelectric properties of polygrained icosahedral $Al_{71-x}Ga_xPd_{20}Mn_9$ ($x = 0, 2, 3, 4$) quasicrystals, J. Appl. Phys. 104 (2008) 073721.
[29] J.M. Dubois, New prospects from potential applications of quasicrystalline materials, Mater. Sci. Eng., A 294–296 (2000) 4–9.
[30] D.J. Sordelet, S.D. Widener, Y. Tang, M.F. Besser, Characterization of a commercially produced Al-Cu-Fe-Cr quasicrystalline coating, Mater. Sci. Eng., A 294–296 (2000) 834–837.
[31] J. Sladek, V. Sladek, S.N. Atluri, Path-independent integral infracture mechanics of quasicrystals, Eng. Fract. Mech. 140 (2015) 61–71.
[32] K. Urban, M. Feuerbacher, M. Wollgarten, Mechanical behavior of quasicrystals, MRS Bull. 22 (1997) 65–68.
[33] S.D. Kaloshkin, V.V. Tcherdyntsev, A.A. Stepashkin, V.N. Gulbin, B.V. Jalnin, A.I. Laptev, et al., Mechanical alloying of metal matrix composites reinforced by quasicrystals, J. Metastable Nanocryst. Mater. 24–25 (2005) 113–116.
[34] R.T. Li, Z.L. Dong, N.W. Khun, K.A. Khor, Novel Ti based metal matrix composites reinforced with Al-Cr-Fe quasicrystals approximants, Mater. Sci. Technol. 31 (2015) 688–694.
[35] R.T. Li, Z.L. Dong, K.A. Khor, Al-Cr-Fe quasicrystals as novel reinforcements in Ti based composites consolidated using high pressure spark plasma sintering, Mater. Des. 102 (2016) 255–263.
[36] S.D. Kaloshkin, V.V. Tcherdyntsev, V.D. Danilov, Preparation of Al-Cu-Fe quasicrystalline powdered alloys and related materials by mechanical activation, Crystallogr. Rep. 52 (2007) 953–965.
[37] P.D. Bloom, J.U. Otaigbe, V.V. Sheares, High-performance quasicrystal-reinforced polymer composites, Proc. Am. Chem. Soc. Div. Polym. Mater.: Sci. Eng. 80 (1999) 406–407.
[38] P.D. Bloom, K.G. Baikerikar, J.U. Otaigbe, V.V. Sheares, Development of novel polymer/quasicrystal composite materials, J. Mater. Sci. Eng. A 294–296 (2000) 156–159.
[39] C. Patino-Carachure, J.E. Froes-Chan, A. Floes Gil, G. Rosas, Synthesis of onion-like carbon-reinforced Al-Cu-Fe quasicrystals by high-energy ball milling, J. Alloy. Comp. 694 (2017) 46–60.
[40] E.A. Golovkova, E.A. Ekimov, A.S. Ivanov, V.S. Kruglov, A.F. Pal, A.N. Ryabinkin, et al., Structure and tribological properties of composite materials based on Al-Cu-Fe formed at high pressure, Tech. Phys. Lett. 43 (2017) 972–975.
[41] T. Bonchina, F. Zupanic, In situ TEM study of precipitation in a quasicrystal-strengthened Al-alloy, Arch. Metall. Mater. 62 (2017) 5–9.
[42] N. Kang, Y. Fu, P. Coddet, B. Guelorget, H. Liao, C. Coddet, On the microstructure, hardness and wear behavior of Al-Fe-Cr quasicrystal reinforced Al matrix composite prepared by selective laser melting, Mater. Des. 132 (2017) 104–111.
[43] A.A. Stepashkin, D.I. Chukov, L.K. Olifirov, A.I. Salimon, V.V. Tcherdyntsev, Quasicrystalline powders as the fillers for polymer-based composites: production, introduction to polymer matrix, properties, in: K.V. Anisimov, A.V. Dub, S.K. Kolpakov, A.V. Lisitsa, A.N. Petrov, V.P. Polukarov, et al. (Eds.), Proceedings of the Scientific-Practical Conference "Research and Development - 2016, Springer, Cham, 2018.
[44] P.D. Bloom, K.G. Baikerikar, J.W. Anderegg, V.V. Sheares, Fabrication and wear resistance of Al-Cu-Fe quasicrystal-epoxy composite materials, Mater. Sci. Eng., A 360 (2003) 46–57.
[45] B.C. Anderson, P.D. Bloom, K.G. Baikerikar, V.V. Sheares, S.K. Mallapragada, Al-Cu-Fe quasicrystal/ultra-high molecular weight polyethylene composites as biomaterials for acetabular cup prosthetics, Biomaterials 23 (2002) 1761–1768.
[46] S. Kenzari, D. Bonina, J.M. Dubois, V. Fournée, Quasicrystal-polymer composites for selective laser sintering technology, Mater. Des. 35 (2012) 691–695.
[47] S.D. Kaloshkin, L.J. Vandi, V.V. Tcherdyntsev, E.V. Shelekhov, V.D. Danilov, Multi-scaled polymer-based composite materials synthesized by mechanical alloying, J. Alloy. Comp. 483 (2009) 195–199.
[48] M.B. Tsetlin, A.A. Teplov, S.I. Belousov, S.N. Chvalun, Y.A. Golovkova, S.V. Krasheninnikov, et al., Tribological and mechanical properties of composites based on ethylene-tetrafluoroethylene and quasicrystalline Al-Cu-Fe filler, J. Surf. Invest. 11 (2017) 315–321.
[49] A. Sakly, S. Kenzari, D. Bonina, S. Corbel, V. Fournée, A novel quasicrystal-resin composite for stereolithography, Mater. Des. 56 (2014) 280–285.
[50] M. Fevzi Ozaydin, H. Liang, Design and synthesis of a geopolymer-enhanced quasicrystalline composite for resisting wear and corrosion, J. Tribol. 138 (2015) 021601–021606.
[51] S. Kenzari, D. Bonina, A. Degiovanni, J.-M. Dubois, V. Fournée, Quasicrystal-polymer composites for additive manufacturing technology, Acta Phys. Pol., A 126 (2014) 449–452.
[52] T.P. dos Santos Barros, D.G. de Lima Cavalcante, D.F. Oliveira, R.E. Caluête, S.J.G. Lima, Study of the surface properties of the epoxy/quasicrystal composite, J. Mater. Res. Technol. (2018), https://doi.org/10.1016/j.jmrt.2018.04.015.
[53] M.B. Tsetlin, A.A. Teplov, S.I. Belousov, S.N. Chvalun, E.A. Golovkova, S.V. Krasheninnikov, et al., Effect of a quasicrystalline filler on the tribological properties of a composite based on ultrahigh-molecular-weight polyethylene, J. Synch. Investig. 9 (2015) 1077–1084.
[54] A. Kothalkar, A.S. Sharma, K. Biswas, B. Basu, Novel HDPE-quasicrystal composite fabricated for wear resistance, Phil. Mag. 91 (2011) 2944–2953.
[55] A. Kothalkar, A.S. Sharma, G. Tripathi, B. Basu, K. Biswas, HDPE-quasicrystal composite: fabrication and wear resistance, Trans. Indian Inst. Met. 65 (2012) 13–20.
[56] M.B. Tsetlin, A.A. Teplov, S.I. Belousov, S.N. Chvalun, E.A. Golovkova, S.V. Krasheninnikov, et al., Composite material based on polytetrafluoroethylene and Al-Cu-Fe quasi-crystal filler with ultralow wear: morphology, tribological, and mechanical properties, J. Synch. Investig. 12 (2018) 277–285.
[57] V.V. Tcherdyntsev, A.A. Stepashkin, D.I. Chukov, L.K. Olifirov, F.S. Senatov, Formation of ethylene-vinyl acetate composites filled with Al-Cu-Fe and Al-Cu-Cr quasicrystallline particles, J. Mater. Res. Technol. (2018), https://doi.org/10.1016/j.jmrt.2018.05.008.
[58] M.B. Tsetlin, A.A. Teplov, S.I. Belousov, S.N. Chvalun, Y.A. Golovkova, S.V. Krasheninnikov, et al., Tribological and mechanical properties of composites based on ethylene-tetrafluoroethylene and quasicrystalline Al-Cu-Fe filler, J. Synch. Investig. 11 (2017) 315–321.
[59] D.I. Chukov, A.A. Stepashkin, V.V. Tcherdyntsev, L.K. Olifirov, S.D. Kaloshkin, Structure and properties of composites based on polyphenylene sulfide reinforced with Al-Cu-Fe quasicrystalline particles, J. Thermoplast. Compos. Mater. 31 (2018) 882–895.
[60] S.M. Aldoshin, G.I. Dzhardimalieva, A.D. Pomogailo, YuA. Abuzin, Reactivity of metal-containing monomers 71.* Synthesis of nanosized quasicrystals and related metallopolymer composites, Russ. Chem. Bull. 60 (2011) 1871–1879.
[61] A.N. Bychkov, G.I. Dzhardimalieva, G.P. Fetisov, V.V. Valskiy, N.D. Golubeva, A.D. Pomogailo, Synthesis and characterization of metal-polymer nanocomposites with radiation-protective properties, Russ. Metallurgy (Metally) (2016) 1207–1213.
[62] A.N. Bychkov, E.A. Sokolov, S.V. Barinov, YuI. Deniskin, K.A. Kydralieva, I.E. Uflyand, et al., Nanocomposite materials based on metal-containing nanoparticles and thermoplastic polymer matrices: production and properties, Int. J. Nanomech. Sci. Technol. 8 (2017) 7–25.
[63] R. Jenkins, R.L. Snyder, Chemical Analysis: Introduction to X-Ray Powder Diffractometry, Wiley, 1996.
[64] X. Xiu, S. Cai, C. Xie, Preparation, structure and thermal stability of Cu nanocomposites, Mater. Chem. Phys. 95 (2006) 122–129.
[65] C.J. Schwartz, S. Bahadur, S.K. Mallapragada, Effect of crosslinking and Pt-Zr quasicrystal fillers on the mechanical properties and wear resistance of UHMWPE for use in artificial joints, Wear 263 (2007) 1072–1080.
[66] E.A. Turi, T.J. Taylor, V.V. Vickroy, R.F. Abbott, Dynamic mechanical relaxations in polyethylene, Macromolecules 18 (1985) 1302–1309.